Foffa, D., Dunne, E. M., Nesbitt, S. J., Butler, R. J., Fraser, N. C., Brusatte, S. L., Farnsworth, A., Lunt, D. J., Valdes, P. J., Walsh, S., & Barrett, P. M. (2022). Scleromochlus and the early evolution of Pterosauromorpha. *Nature*, *610*(7931), 313-318. https://doi.org/10.1038/s41586-022-05284-x

Scleromochlus and the early evolution of Pterosauromorpha

Davide Foffa[1,2,3*], Emma M. Dunne[2], Sterling J. Nesbitt[3], Richard J. Butler[2], Nicholas C. Fraser[1,4], Stephen L. Brusatte[4,1], Alexander Farnsworth[5,6,7], Daniel J. Lunt[7], Paul J. Valdes[7], Stig Walsh[1,4], Paul M. Barrett[8]

[1]Department of Natural Sciences, National Museums Scotland, Chambers Street, Edinburgh EH1 1JF, UK

[2]School of Geography, Earth and Environmental Sciences, University of Birmingham, Edgbaston, Birmingham B15 2TT, UK

[3]Department of Geosciences, Virginia Tech, 4044 Derring Hall (MC0420) 926 West Campus Drive, Blacksburg, Virginia 24061, USA

[4]School of GeoSciences, University of Edinburgh, Grant Institute, Hutton Road, Edinburgh EH9 3FE, UK

[5]State Key Laboratory of Tibetan Plateau Earth System, Resources and Environment (TPESRE), Institute of Tibetan Plateau Research, Chinese Academy of Sciences, Beijing, 100101, China

[6]Key Laboratory of Continental Collision and Plateau Uplift, Institute of Tibetan Plateau Research, and Center for Excellence in Tibetan Plateau Earth Sciences, Chinese Academy of Sciences, Beijing 100101, China

[7]School of Geographical Sciences, University of Bristol, University Road, Bristol, BS8 1SS, UK

[8]Natural History Museum, Cromwell Road, London SW7 5BD, UK

*corresponding author: d.foffa@nms.ac.uk

Pterosaurs, the first vertebrates to evolve powered flight, were key components of Mesozoic terrestrial ecosystems, from their sudden appearance in the Late Triassic until their demise at the end of the Cretaceous[1–6]. However, the origin and early evolution of pterosaurs are poorly understood, due to a substantial stratigraphic and morphological gap between these reptiles and their closest relatives[6], Lagerpetidae[7]. *Scleromochlus taylori*, a tiny reptile from the early Late Triassic of Scotland discovered over a century ago, was hypothesized to be a key taxon closely related to pterosaurs[8], but its poor preservation has limited prior studies and resulted in controversy over its phylogenetic position, with some even doubting its identification as an archosaur[9]. Here we use micro-computed tomographic scans to provide the first accurate whole skeleton reconstruction and a revised diagnosis of *Scleromochlus*, revealing new anatomical details that conclusively identify it as a close pterosaur relative[1] within Pterosauromorpha (the lagerpetid + pterosaur clade). *Scleromochlus* is anatomically more similar to lagerpetids than to pterosaurs and retains numerous features that were likely present in very early diverging members of Avemetatarsalia (bird-line archosaurs). These results support the hypothesis that the first flying reptiles evolved from tiny, likely facultatively bipedal, cursorial ancestors[1].

Pterosaurs were iconic components of Mesozoic (~252–66 million years ago) ecosystems and the first group of vertebrates to achieve powered flight, with a fossil record spanning over 150 million years, from the Late Triassic until the end of the Cretaceous[2–3,6]. However, our understanding of the origin and early evolution of pterosaurs is hindered by major stratigraphic and morphological gaps between these highly modified reptiles and their closest relatives[6–7]. Even at the time of their first appearance ~220 million years ago (middle Norian, Late Triassic), the pterosaur body plan was so specialized that the identity of their closest relatives has long been mysterious[2–3,6–7]. Recently, lagerpetids – a group of small-bodied, terrestrial archosaurs previously thought to be close to dinosaur ancestry – were shown to be the sister taxon of pterosaurs, together forming Pterosauromorpha[7]. This discovery reduced the anatomical distance between pterosaurs and their close relatives but left unanswered many questions regarding the tempo and mode of the morphological transformations occurring during the origin of pterosauromorphs[6].

Scleromochlus taylori, known from seven articulated skeletons from the Upper Triassic Lossiemouth Sandstone Formation of Scotland[1,4–5,8,12], has been considered central to resolving the origin of pterosaurs[1,4,5,8]. However, the anatomy and phylogenetic position of this reptile have been controversial because its small size – less than 20 cm in total length – and unusual preservation mode, as voids in sandstone, have made interpreting its osteology challenging[1,4–5,8,12]. Previous anatomical studies of *Scleromochlus* have relied primarily on casts of natural moulds of the skeletons. While such casts were long necessary, their ability to capture tiny, but crucial, anatomical details has been questioned and the reliability of the interpretations based upon them are debated[4–5,9,13–14].

Since its discovery in 1907[12], the anatomy of *Scleromochlus* has been redescribed in detail four times[1,5,8–9], in addition to many other discussions on its mode of life and relationships (e.g.[3–4,13] among others, Supplementary Information). Thanks to these studies,

68 the general anatomy of *Scleromochlus* is well-known: it had a large head, short neck, gracile
69 body and long hind limbs. Many other phylogenetically critical details are still unclear, such
70 as the orientation of the quadrate, presence/absence of the mandibular fenestra, relative
71 lengths of the forelimb segments, proportions of the torso, interpretation of the ankle, length
72 of the tail, and whether the body was covered in osteoderms. Before synapomorphy-based
73 studies, *Scleromochlus* was usually considered to be either a dinosaur[12] or a crocodile-line
74 pseudosuchian[8] (see Supplementary Information); since the advent of phylogenetic analyses
75 based on cladistic principles, *Scleromochlus* has been recovered as either a non-archosaurian
76 archosauromorph[9] or more frequently as an avemetatarsalian[5,15], close either to
77 dinosauromorphs[4–5,15] or pterosaurs[1,4–5,7,15,17] (Supplementary Information).
78 Here, using microcomputed tomographic (μCT) techniques, we provide substantial
79 new, formerly inaccessible, information on the anatomy of *Scleromochlus*, including critical
80 regions and previously unknown elements. This approach allowed us to construct a revised
81 taxonomic diagnosis, clarify the phylogenetic relationships of *Scleromochlus* and build the
82 first accurate three-dimensional skeletal reconstruction of this pivotal taxon (Figs. 1–4,
83 Extended Data Figs. 1–2, Supplementary Information videos 1–6).
84 Our μCT data demonstrates that prior knowledge of *Scleromochlus* anatomy was
85 incomplete and, in some cases, misleading. Traditional casting techniques failed to
86 adequately capture crucial details of the skull, mandible, long bones and ribs, and did not
87 provide access to important sections of the skeleton (e.g. tail, manus, pes). The μCT scans
88 greatly increase the available information from all seven known individuals (Fig. 1), enabling
89 us to demonstrate that *Scleromochlus* possesses cranial and postcranial character states
90 diagnostic of pterosauromorphs (Fig. 2) and a previously unrecognised series of features that
91 are common in early bird-line archosaurs.

92 **Description.** None of the *Scleromochlus* specimens are highly distorted but most
93 display at least some post-mortem disarticulation[5,9,13] (i.e. displaced or missing small body
94 parts) and compression (Supplementary Information). Previous authors proposed that the
95 cranium had a long, low profile in life[5,9], and this observation was used to support the
96 hypothesis that *Scleromochlus* is a doswelliid[9] – a stem archosaur just outside the crown
97 group. However, µCT data show that disarticulation and flattening of the skeletons was
98 underestimated in previous studies, suggesting that the skulls were dorsoventrally
99 compressed taphonomically and would have been considerably deeper in life. Skull length is
100 ~50% that of the presacral vertebral column, as in early pterosaurs[1,4–5,8] (and potentially
101 lagerpetids), but unlike those of other early avemetatarsalians, which have proportionally
102 smaller heads[15]. The maxilla has an anterior process that tapers to a point and a concave
103 anterior margin, which is a synapomorphy of pterosauromorphs[7] (Figs. 1a, 2a–c). A newly
104 imaged quadrate has a weakly concave posterior surface (Fig. 1b) and is vertically[9] to slightly
105 posteroventrally-to-anterodorsally oriented as in most Triassic archosaurs, contrary to
106 previous assessments[5,12] of an anteroventrally-to-posterodorsally oriented quadrate similar to
107 those characterising early pterosaurs[6–7] and some aetosaurs[16]. The basioccipital neck is very
108 short, as in lagerpetids and early pterosaurs[7]. µCT data confirm the debated[5,9] presence of a
109 well-developed external mandibular fenestra (Fig. 1b), as in most archosauriforms[17–19] and,
110 uniquely amongst pterosaurs, the Triassic taxon *Austriadraco dallavecchiai*[20]. The
111 retroarticular process of the lower jaw extends well posterior to the glenoid fossa[6], as in many
112 early pterosaurs[6,20], rather than being short[9] (Fig.1b).
113 In the vertebral column, the short cervical centra[4,8] result in a neck that is
114 proportionately shorter than those of pterosaurs, aphanosaurs, and other early
115 avemetatarsalians[15,21]. The centra of the dorsal vertebrae[5,12] increase in length from the
116 shoulders to the pelvis (Fig. 1c). The middle and posterior dorsal centra are uniquely

117 elongated for an archosaur (see Table 4 in[23]), with a centrum length/height ratio of >2.5,
118 contributing to a torso that is similar in proportional length to those of silesaurids and
119 aphanosaurs[15,21–22], a similarity that may not be immediately noticeable because of the
120 extreme elongation of the limbs in *Scleromochlus*. The dorsal ribs are 3–4 times longer than
121 previous estimates (Fig. 1c), showing that the torso is deep, and not dorsoventrally flattened[9].
122 The number of sacral vertebrae is unclear but it is likely that there were either two, or no
123 more than three, based on the lengths of the centra relative to the ilium. The tail of
124 *Scleromochlus* has a minimum of ~50 caudal vertebrae, based on newly exposed caudal
125 segments in three specimens. This corroborates earlier research[8,12] and a recent redescription[9],
126 and contrasts with other assessments that reported an unusually short tail[4–5]. We did not find
127 evidence for any three-dimensional structures dorsal to the vertebrae that would indicate the
128 presence of osteoderms; the two-dimensional structures previously identified as
129 osteoderms[5,9,13] may be integument impressions instead.
130 The scapular blade is thin[5,9,12] and long, with an anteriorly concave margin and a
131 weakly flared distal end (Fig. 1e). The limbs are comparatively longer and slenderer than
132 those of any other Triassic avemetatarsalian[23–24]. The humerus has a straight shaft, a small
133 deltopectoral crest, an expanded distal end, and is confirmed as longer than either the radius
134 or ulna (Fig. 1e–f; Extended Data Fig. 2, Extended Data Table 1), as in lagerpetids, but unlike
135 pterosaurs[7]. The metacarpus of *Scleromochlus* is short, less than 10% of total humeral length,
136 and the manus is small (Fig. 1f–g, Extended Data Fig. 2, Extended Data Table 1), which is
137 distinct from the elongated hands of other pterosauromorphs[7]. The ilium is similar to those of
138 lagerpetids in its relatively small size compared to the length of the hindlimb, and has an
139 expanded pre-pubic peduncle that is dorsally concave above the acetabulum[7] and extends
140 anteriorly beyond a pre-acetabular process, which is not as well developed as those in
141 pterosaurs (Fig. 1i). The femur has a hook-shaped proximal head[4], which *Scleromochlus*

142 shares with lagerpetids and the earliest-branching pterosaurs[7] (Figs. 1i, 2f–i), and the distal
143 end has a bulbous crista tibiofibularis that is diagnostic of Lagerpetidae[7,11,25–26] (Fig. 2h–m).
144 Interpretations of the ankle structure in *Scleromochlus* have been central to
145 consideration of its phylogenetic affinities[1,4–5,9,12]. However, even with μCT data, we could
146 not satisfactorily clarify the morphology of the ankle components. We therefore opt for a
147 conservative approach and recommend that ambiguous characters of the ankle should be left
148 unscored in phylogenetic analyses. Nonetheless, we also consider previous interpretations of
149 the ankle morphology in our phylogenetic analyses by adopting three separate scoring
150 strategies for *Scleromochlus* (Methods) (Fig. 3, Extended Data Figs. 3–7, Supplementary
151 Information): (i) advanced fused mesotarsal ankle[1]– but with an astragalocalcaneum that is
152 unfused to the tibia and fibula (the latter feature cannot be positively assessed in casts, but
153 there is separation between the proximal tarsals and the distal end of the tibia in the casts and
154 μCT data), similar to the condition in lagerpetids[7]; (ii) "intermediate" mesotarsal ankle[5] with
155 a separate astragalus and calcaneum; and (iii) crurotarsal ankle[8,9,12], the most plesiomorphic
156 option, as in crocodile-line archosaurs (Fig. 3b–g) (see Phylogenetic analyses below and
157 Supplementary Information). We do not see any evidence of four distal tarsals capping the
158 metatarsals in any specimen using μCT data and interpret the previously reported presence of
159 four distal tarsals in NHMUK PV R3556[5,9] as the proximal ends of the metatarsals.
160 The complete pes, described here for the first time, further underlines similarities with
161 lagerpetids (e.g. *Lagerpeton*[27]) (Figs. 1k–l, 2n–p). The foot is proportionally longer than
162 previously reported, and the combined length of the metatarsal + longest digit (IV) surpasses
163 that of the tibia. The proximal and distal pedal phalanges are elongated and subequal in size.
164 The pedal digits decrease in length from IV to I, and digit III is slightly angled relative to the
165 midline, as also occurs in *Lagerpeton*[28]. Because metatarsals I–IV are closely appressed and
166 subequal in length[1,5,8–9,12], the metatarsal-phalangeal joints I–IV are aligned, so that digits I

and II are more prominent in *Scleromochlus* than *Lagerpeton*[27]. The pes has a phalangeal formula of 2-3-4-5-0, as in *Lagerpeton* and early dinosauromorphs[28], differing from the 2-3-4-5-2 formula of early pterosaurs[28] (Fig. 2n–p). The pedal unguals are similar to those of *Lagerpeton*: triangular in cross-section, mediolaterally compressed and, unlike those of most early pterosaurs[6–7], lack recurvature and ventral tubercles (Fig. 1l).

Phylogenetic analyses. New anatomical information from the μCT scans was used to re-score *Scleromochlus* in the largest and best documented phylogenetic data matrix of Permian–Triassic archosauromorphs[7]. This dataset includes taxa relevant to all of the previously hypothesized phylogenetic positions of *Scleromochlu*s and has the largest available sampling of early pterosauromorphs[7] (Methods). Maximum parsimony and Bayesian inference analyses place *Scleromochlus* in Archosauria, Avemetatarsalia and Ornithodira, and its position in Pterosauromorpha is strongly supported by a minimum of eight unambiguous synapomorphies: the base of the ascending process of the maxilla is concave (Character 59, state 1); the occipital neck is extremely short (Character 231, state 1); the metacarpal I is slender (distal end width versus total length <0.33) (Character 448, state 0); presence of a concavity on the dorsal margin of the iliac blade (Character 466, state 2); the pubis is less than 50% the length of the femur (Character 472, state 0/1); the femoral head is distinctly in-turned with respect to the shaft (Character 492, state 1) and 'hook-shaped' (Character 800, state 1); and the length of metatarsal V is less than half length of metatarsal III (Character 823, state 1). *Scleromochlus* also shares the following ambiguous synapomorphy with pterosauromorphs: the skull total length is over half the length of the presacral vertebral column (Character 2, state 1). All analyses, except one, recover *Scleromochlus* in Lagerpetidae, as the earliest diverging species within the group (Fig. 3, Extended Data Figs. 3–6, Supplementary Information). In the maximum parsimony analysis hypothesis where a 'crurotarsal ankle'[8–9] interpretation is scored, we find *Scleromochlus* as

192 the sister taxon to Pterosauria and Lagerpetidae (Supplementary Information). Regardless,
193 *Scleromochlus* is not excluded from Avemetatarsalia even when scored as possessing a
194 crurotarsal ankle – a suite of character states that is also present in aphanosaurs and some
195 dinosauriforms[15] (as well as pseudosuchians). In sum, there is strong evidence placing
196 *Scleromochlus* close to the origin of Pterosauromorpha, and the taxon has a combination of
197 plesiomorphic features that are widespread in early avemetatarsalian groups (aphanosaurs and
198 silesaurids), as well as derived character states that are either diagnostic of pterosauromorphs,
199 lagerpetids or unique to *Scleromochlus*.

200 **Mode of life.** Debate about the locomotor abilities of *Scleromochlus* has confounded
201 our understanding of the lifestyles of close pterosaur relatives. *Scleromochlus* has been
202 described as a digitigrade bipedal runner or leaping saltator[5,12], a sprawling (semi-)digitigrade
203 quadruped, and a frog-like hopper[9], among other locomotor modes. Below we focus on the
204 osteological features supporting or refuting each hypothesis, stressing that all functional
205 inferences should be verified through comprehensive biomechanical testing[29].

206 μCT data show that features considered to support quadrupedality, a sprawling
207 posture and frog-like hopping[9] either derive from misinterpretations of incomplete data (e.g.
208 short ribs, flattened torso and head, stiff osteoderm cuirass covering the sacrum, none of
209 which are present, as shown here), are ambiguous (e.g. ankle structure, narrow foot), or do
210 not appropriately account for disarticulation and taphonomy (the specimens are not likely
211 preserved in *in-vivo* resting poses, as postulated[9]). *Scleromochlus* also lacks unambiguous
212 adaptations for climbing/arboreal behaviour (e.g. recurved claws, elongated fingers), as
213 shown by its slender limbs, small hands and straight pedal claws[7] — but note that small
214 tetrapods can climb without possessing distinct adaptations for this behaviour. The small
215 pelvic girdle is unsuitable for saltatorial (= leaping) behaviour[5,12], which generally requires a
216 reinforced pelvis and enlarged muscle attachments, even in tiny taxa (e.g. birds, frogs,

217 jerboas). Furthermore, other features occasionally used to support saltatorial/hopping
218 locomotion (e.g. a comparatively short trunk, proportions of the hind limb segments,
219 asymmetrical foot) are also common traits of bipedal runners[33]. We conclude that the hind
220 limb morphology and proportions of *Scleromochlus* better support the view that it was
221 digitigrade[1,23,30.], and we were unable to verify traits previously argued to support a
222 plantigrade foot posture (e.g. crurotarsal ankle[8,9], narrow feet[9], lack of metatarsal
223 adaptations[9], hip and femur adaptations[9]).

224 However, even with these new data, uncertainty remains over the posture of
225 *Scleromochlus* because of its unusual body plan. In particular, the forelimb/hind limb ratio
226 (~0.59, similar to the value reported by[23]) falls between those of quadrupedal and bipedal
227 archosauromorphs[1,31], as does the difference between its femoral and humeral diameters[32].
228 The elongate centra of the mid-posterior dorsal vertebrae suggest quadrupedality[23], but the
229 ratios between the hind limb/trunk (~1.6–1.9), and forelimb and hind limb segments to gleno-
230 acetabular distance (~2.41) imply a posteriorly positioned centre of mass, which characterises
231 bipedal archosaurs[23,33]. The ratio between metatarsal and femoral lengths (~0.60) is firmly in
232 the range of efficient runners[31]. Individually these metrics can be confusing, but their co-
233 occurrence is phylogenetically and functionally informative[23]. Overall, we conclude that
234 *Scleromochlus* was a gracile, digitigrade ground-dwelling runner[1], capable of moving in an at
235 least facultative bipedal posture.

236 **Palaeoecological implications.** Because it is the oldest known non-pterosaur
237 pterosauromorph from the Northern Hemisphere, *Scleromochlus* is fundamental to
238 understanding early pterosauromorph evolution. Lagerpetids and pterosaurs rarely co-occur
239 in the same localities[11]: most early pterosaurs are found in the Norian–Rhaetian low-latitude
240 coastal habitats of the Northern Tethyan region, with the exceptions of a yet undescribed
241 pterosaur from the upper Chinle Formation of North America[34], *Caelestiventus*[35] from desert

deposits in North America, *Arcticodactylus* from fluvial facies in Greenland[20,36], *Yelaphomte* and *Pachagnathus* from floodplain/alluvial sediments in Argentina[37]. By contrast, lagerpetids have a wider latitudinal and geographical spread[11], and occur earlier in the stratigraphic record (e.g. Ladinian–Carnian for *Kongonaphon*)[26]. The minimal geographical overlap of the two groups, even during their long stratigraphic overlap in the Norian–Rhaetian, could indicate latitudinal partitioning linked to climate preferences or tolerances. As currently known, the distribution of Triassic pterosauromorphs implies the possibility that climate shaped the early evolution of the clade, and that the biogeographical expansion of the group might have been enabled by the removal of low latitude climatic barriers, such as those following the onset of the Carnian Pluvial Event[38–40]. However, the uneven geographical and temporal sampling of pterosauromorphs, uncertainties in climate models and proxy data (e.g.[10,41–43]), taphonomy[44] and other sampling biases[45], will need to be addressed in order to test these hypotheses rigorously.

Conclusions. New μCT scans have revealed novel anatomical features that conclusively place *Scleromochlus* within Pterosauromorpha, establishing the importance of this historic taxon for understanding the early evolution of the clade. The available evidence suggests that *Scleromochlus* is more closely related to lagerpetids than to pterosaurs, and that it lacks adaptations for either flying, arboreality or a saltatorial lifestyle. Instead, its unusual proportions and hind limb morphology support the hypothesis that the common ancestor of pterosaurs and lagerpetids was a tiny, likely digitigrade, ground-dwelling (potentially bipedal) runner[1] rather than a sprawling quadruped, frog-like hopper or saltator[9]. The lack of flight-related adaptations in *Scleromochlus* and lagerpetids suggests that the evolution of the distinctive pterosaurian body-plan remains to be found in the ~18 Mya gap between the first pterosaurs and the origin of pterosauromorphs[7].

1. Padian, K. The origin of pterosaurs. In: Reif W-E, Westphal F, *eds. Third Symposium on Mesozoic Terrestrial Ecosystems, Short Papers. Tübingen: Attempto*, 163–168 (1984).
2. Padian, K. The origins and aerodynamics of flight in extinct vertebrates. *Palaeontology* **28**, 413–433 (1985).
3. Witton, M. P. *Pterosaurs: Natural History, Evolution, Anatomy* (Princeton Univ. Press, 2013).
4. Sereno, P. C. Basal archosaurs: phylogenetic relationships and functional implications. *Soc. Vertebr. Paleontol. Mem.* **2**, 1–53 (1991).
5. Benton, M. J. *Scleromochlus taylori* and the origin of dinosaurs and pterosaurs. *Phil. Trans. R. Soc. Lond. B* **354**, 1423–1446 (1999).
6. Dalla Vecchia, F.M. 2013. Triassic pterosaurs. In *Anatomy, Phylogeny and Palaeobiology of Early Archosaurs and their Kin* (eds Nesbitt, S. J. et al.) 119–155 (Geological Society London 2013).
7. Ezcurra, M.D., Nesbitt, S.J., Bronzati, M. *et al.*. Enigmatic dinosaur precursors bridge the gap to the origin of Pterosauria. *Nature* 588, 445–449 (2020).
8. Huene, F. von. 1914. Beiträge zur Geschichte der Archosaurier. Geologische und Palaeontologische Abhandlungen, Neue Folge 13: 1–53.
9. Bennett, S. C. Reassessment of the Triassic archosauriform *Scleromochlus taylori*: neither runner nor biped, but hopper. *PeerJ* **8**, e8418 (2020).
10. Dunne, E. M., Farnsworth, A., Greene, S. E., Lunt, D. J., Butler, R. J. Climatic drivers of latitudinal variation in Late Triassic tetrapod diversity. *Palaeontology*, **64**, 101–117 (2020).

11. Müller, R.T., Langer, M.C., Dias-da-Silva, S. Ingroup relationships of Lagerpetidae (Avemetatarsalia: Dinosauromorpha): a further phylogenetic investigation on the understanding of dinosaur relatives. *Zootaxa* **4392(1)**, 149–158 (2018).
12. Woodward, A. S. On a new dinosaurian reptile (*Scleromochlus Taylori*, gen. et sp. nov.) from the Trias of Lossiemouth, Elgin. *Q. J. Geol. Soc. Lond.* **63(1–4)**,140–144 (1907).
13. Benton, M. J., Walker, A. D. Palaeoecology, taphonomy, and dating of Permo-Triassic reptiles from Elgin, north-east Scotland. *Palaeontology* **28,** 207–234 (1985).
14. Foffa, D., Butler, R. J., Nesbitt, S. J., Walsh, S., Barrett, P. M., Brusatte, S. L., Fraser, N. C. 2020. Revision of *Erpetosuchus* (Archosauria: Pseudosuchia) and new erpetosuchid material from the Late Triassic 'Elgin Reptile' fauna based on μCT scanning techniques. *Earth Environ. Sci. Trans. R. Soc. Edinb.* **111(4)**, 209–233. (2020).
15. Nesbitt, S. J., Butler, R. J., Ezcurra, M. D., Barrett, P. M., Stocker, M. R., Angielczyk, K. D., Smith, R. M. H., Sidor, C. A., Niedźwiedzki, G., Sennikov, A. G., Charig, A. J. The earliest bird-line archosaurs and the assembly of the dinosaur body plan. *Nature* **544(7651)**, 484–487 (2017).
16. Desojo, J. B., Heckert, A. B., Martz, J. W., Parker, W. G., Schoch, R. R., Small, B. J., Sulej, T. 2013. Aetosauria: a clade of armoured pseudosuchians from the Upper Triassic continental beds. In *Anatomy, Phylogeny and Palaeobiology of Early Archosaurs and their Kin* (eds Nesbitt, S. J. et al.) 203–239 (Geological Society London 2013).
17. Gauthier, J. A. (1986). Saurischian monophyly and the origin of birds. In Padian, K. The Origin of Birds and the Evolution of Flight, Memoirs of the California Academy of Sciences 8. California Academy of Sciences, 1–55.

18. Nesbitt, S. J. The early evolution of archosaurs: relationships and the origin of major clades. *Bull. Am. Mus. Nat. Hist.* **352**, 1–292 (2011).
19. Ezcurra, M. D. The phylogenetic relationships of basal archosauromorphs, with an emphasis on the systematics of proterosuchian archosauriforms. **PeerJ 4**, e1778 (2016).
20. Kellner A.W.A. Comments on Triassic pterosaurs with discussion about ontogeny and description of new taxa. *An. Acad. Bras. Cienc.* **87(2)**, 669–689 (2015).
21. Dzik, J. A beaked herbivorous archosaur with dinosaur affinities from the early Late Triassic of Poland. *J. Vertebr. Paleontol.* **23**, 556–574 (2003).
22. Yáñez, I., Pol, D., Leardi, J. M., Alcober, O. A., Martínez, R. N. 2021. An enigmatic new archosauriform from the Carnian–Norian, Upper Triassic, Ischigualasto Formation of northwestern Argentina. *Acta Palaeontol. Pol.* **66(3)**, 509–533 (2021).
23. Padian, K. Were pterosaur ancestors bipedal or quadrupedal?: morphometric, functional, and phylogenetic considerations. *Zitteliana*, **B28**, 21–33 (2008).
24. McCabe, M. B., Mason, B., Nesbitt, S. J. The first pectoral and forelimb material assigned to the lagerpetid *Lagerpeton chanarensis* (Archosauria: Dinosauromorpha) from the upper portion of the Chañares Formation, Late Triassic. *Palaeodiversity* **14**, 121–131 (2021).
25. Irmis, R.B., Nesbitt, S.J., Padian, K., Smith, N.D., Turner, A.H., Woody, D., Downs, A. A late Triassic dinosauromorph assemblage from New Mexico and the rise of dinosaurs. *Science* **317(5836)**, 358–361 (2007).
26. Kammerer, C. F., Nesbitt, S. J., Flynn, J. J., Ranivoharimanana, L., Wyss, A. R. A tiny ornithodiran archosaur from the Triassic of Madagascar and the role of miniaturization in dinosaur and pterosaur ancestry. *Proc. Natl. Acad. Sci.* USA 117, 17932–17936 (2020).

27. Sereno, P. C., Arcucci, A. B. Dinosaurian precursors from the Middle Triassic of Argentina: *Lagerpeton chanarensis*. *J. Vertebr. Paleontol.* **13(4)**, 385–399 (1994).

28. Hone, D. W. E., Tischlinger, H., Frey, E., Röper, M. A New Non-Pterodactyloid Pterosaur from the Late Jurassic of Southern Germany. *PLoS ONE* **7(7)**, e39312 (2012).

29. Demuth, O. E., Rayfield, E. J., Hutchinson, J. R. 3D hindlimb joint mobility of the stem-archosaur Euparkeria capensis with implications for postural evolution within Archosauria. *Sci. Rep*. **10**, 15357 (2020).

30. Padian, K. A functional analysis of flying and walking in pterosaurs. *Paleobiology* **9(3)**, 218–239 (1983).

31. Kubo, T., Kubo, M. O. Associated evolution of bipedality and cursoriality among Triassic archosaurs: a phylogenetically controlled evaluation. *Paleobiology* **38(3)**, 474–485. (2012).

32. Campione, N. E., Evans, D. C., Brown, C. M. and Carrano, M. T. Body mass estimation in non-avian bipeds using a theoretical conversion to quadruped stylopodial proportions. *Methods Ecol Evol* 5, 913-923 (2014).

33. Barrett, P.M., Maidment, S.C.R. The evolution of ornithischian quadrupedality. *J. Iber. Geol.* **43**, 363–377 (2017). https://doi.org/10.1007/s41513-017-0036-0

34. Britt, B.B., Dalla Vecchia, F.M., Chure, D.J., Engelmann, G.F., Whiting, M.F., Scheetz, R.D. *Caelestiventus hanseni* gen. et sp. nov. extends the desert-dwelling pterosaur record back 65 million years. *Nat. Ecol. Evol.* **2(9)**, 1386–1392 (2018).

35. Behrensmeyer, A. K., Whatley, R. L., Fitch, A. J., Parker, W., McIntire, S., Pritchard, A. C., Klingman, B., Cline, R. G. Taphonomy and paleocommunity reconstruction of a pterosaur-bearing fossil assemblage in the Upper Triassic of Arizona. *Journal of Vertebrate Paleontology, Program and Abstracts*, 2019, 61.

36. Jenkins F.A. Jr., Shubin N.H., Gatesy S.M. and Padian K. A diminutive pterosaur (Pterosauria: Eudimorphodontidae) from the Greenlandic Triassic. *Bull. Mus. Comp. Zool.* **156**, 151–170 (2001).

37. Martínez, R. N., Andres, B., Apaldetti, C., Cerda, I.A. The dawn of the flying reptiles: first Triassic record in the southern hemisphere. *Pap. Palaeontol.* **8**: e1424 (2022). https://doi.org/10.1002/spp2.1424

38. Simms, M. J., Ruffell, A. H. Synchroneity of climatic change and extinctions in the Late Triassic. *Geology,* **17(3)**, 265–268 (1989) doi: https://doi.org/10.1130/0091-7613(1989)017<0265:SOCCAE>2.3.CO;2

39. Roghi, G., Gianolla, P., Minarelli, L., Pilati, C., Preto, N. Palynological correlation of Carnian humid pulses throughout western Tethys. *Palaeogeography, Palaeoclimatology, Palaeoecology* **290**, 89–106 (2010).

40. Benton, M. J., Bernardi, M., Kinsella, C. The Carnian Pluvial episode and the origin of dinosaurs. *J. Geol. Soc.* **175**, 1019–1026 (2018).

41. Liu, J., Angielczyk, K. D., Abdala, F. Permo-Triassic tetrapods and their climate implications. *Glob. Planet. Change* **205**, 103618 (2021).

42. Chiarenza, A. A., Mannion, P. D., Farnsworth, A., Carrano, M., Varela, S. Climatic constraints on the biogeographic history of Mesozoic dinosaurs. Current Biology , 32 (3) pp. 570-585 (2022) doi: 10.1016/j.cub.2021.11.061.

43. Mancuso, A. C., Irmis, R. B., Pedernera, T. E., Gaetano, L. C., Benavente, C. A., Breeden, III, B. T. Paleoenvironmental and Biotic Changes in the Late Triassic of Argentina: Testing Hypotheses of Abiotic Forcing at the Basin Scale. Front. Earth Sci. 10:883788 (2022) doi: 10.3389/feart.2022.883788

44. Kellner, A.W.A. Remarks on pterosaur taphonomy and paleoecology. *Acta Geol. Leopold.* **39**, 175–189 (1994).

45. Dean, C.D., Mannion, P.D. and Butler, R.J. Preservational bias controls the fossil record of pterosaurs. *Palaeontology* **59**, 225-247 (2016).

Figures

Figure 1. Newly revealed anatomical features of *Scleromochlus taylori*. **a**, NHMUK PV R3557, skull in dorsolateral view. **b**, NHMUK PV R3557, right quadrate (blue), posterior lower jaw (green) and ceratobranchial bone (purple) in posterodorsal view. **c,** NHMUK PV R3557, torso and rib cage in ventral view. **d,** NHMUK PV R3556, caudal vertebrae in lateral view (mirrored). (**e**) NHMUK PV R3556, distal end of the left humerus in oblique posterior-medial view and dorsal view of the left scapula. **f,** NHMUK PV R3557, right forearm and hand in medial view. **g,** reconstruction of the hand (composite) in dorsal view. **h**, NHMUK PV R3557, partially exposed left ilium in lateral view. **i**, NHMUK PV R3557, proximal right femur in medial view. **j**, NHMUK PV R3146, distal end of the right femur in distal view. **k**, NHMUK PV R3914, right hindlimb in ventral view. **l**, NHMUK PV R3914, details of the last phalanges and unguals of pedal digit II and III in lateral view. **m** Skeletal reconstruction of *Scleromochlus taylori*, red shading indicates areas that most benefited from μCT data. Scale bars equal 10 mm (**a**, **c**, **e**, **f**, **h**); 5 mm (**b**, **k**, **l**); 2 mm (**i**, **j**). See Methods for abbreviations.

Figure 2. Comparisons of selected features of *Scleromochlus taylori* and pterosauromorphs. **a**–**c**, Right maxilla in lateral view: **a**, *Scleromochlus taylori* (NHMUK PV R3557); **b**, *Kongonaphon kely* (UA 10618); **c**, *Raeticodactylus filisurensis* (BNM 14524). **d**–**g**, Proximal end of the right femur in posteromedial view: d, *Scleromochlus taylori* (NHMUK PV R3557); **e**, *Lagerpeton chanarensis* (PVL 4619); **f**, *Dromomeron gregorii* (TMM-31100-1306); **g**, *Raeticodactylus filisurensis* (BNM 14524, reversed). **h**–**m**, Distal ends of the right femora of pterosauromorphs in posterior (**h**) and distal views (**i–m**): **h**, *Scleromochlus taylori* (NHMUK PV R3146); **i**, *Scleromochlus taylori* (NHMUK PV R3557); **j**, *Scleromochlus taylori* (NHMUK PV R3556); **k**, *Lagerpeton chanarensis* (PVL 4619); **l**, *Dromomeron gregorii* (TMM-31100-1306); **m**, *Dromomeron romeri* (GR 218). (**n**–**p**)

Pterosauromorph left foot in dorsal view: **n**, *Scleromochlus taylori*; **o**, *Lagerpeton chanarensis* (redrawn from[26]); **p**, generic Triassic pterosaur (redrawn from[39]). Scale bars equal 10 mm (**a**–**c**, **e**–**g**, **n**–**p)**, 2 mm (**d**, **h**–**j)**. See Methods for abbreviations.

Figure 3. Time-calibrated strict consensus tree focused on Pterosauromorpha and different positions of *Scleromochlus taylori* based upon interpretations of the phylogenetic scores for the ankle. a, time calibrated strict consensus tree of Archosauria focused on Pterosauromorpha (for complete versions and branch support values, see Extended Data Figs. 3–7). **b**–**c**, advanced mesotarsal ankle interpretation (= fused astragalocalcaneum). **d**–**e**, "intermediate" mesotarsal ankle interpretation. **f**–**g**, crurotarsal ankle interpretation. Note the different interpretation and position of the astragalus, calcaneum and tarsals (i–iii). The grey '?' in panel **a** represents our recommended scoring strategy: 'unscored ankle'. Scale bars equal 5 mm in b–g. See main text for abbreviations. Silhouettes by Scott Hartman from www.phylopic.org, covered by https://creativecommons.org/licenses/by/3.0/, used with permission.

Figure 4. Digital 3D life reconstruction of *Scleromochlus taylori*. a, Digital 3D model, created by Matt Humpage based on µCT data. **b,** life reconstruction by Gabriel Ugueto. Scale bar equals 50 mm. [1.5 column-width]

Methods

Anatomical abbreviations: aeg, anterior extensor groove; **aof**, antorbital fossa; **ar**, articular; **as,** astragalus; **asf**, astragalar facet; **ast**, tubercle on astragalus; **c**, carpal; **ca**, calcaneum; **cat**, calcaneal tuber**; c,** carpal; **ctf**, crista tibiofibularis; **emf**, external mandibular fenestra; **en**, external naris; **fe**, femur; **hy**, hyoid; **il**, ilium; **lco**, lateral condyle; **le**, lateral emargination; **mc I-V**, metatarsals I to IV; **mco**, medial condyle; **mt**, metatarsal**; mx**, maxilla; **ph**, phalanx; **pmx**, premaxilla; **poz**, postzygapophysis; **prz**, prezygapophysis; **q**, quadrate; **qj**, quadratojugal; **ra**, radius; **rap**, retroarticular process; **sc**, scapula; **sk**, skull fragment; **t**, tarsal; **ti**, tibia; **ul**, ulna.

Institutional abbreviations: BNM, Bündner Naturmuseum, Chur (Switzerland); **GR**, Ghost Ranch Ruth Hall Museum of Paleontology, Abiquiú, NM (USA); **NHMUK,** Natural History Museum, London (United Kingdom); **PVL**, Paleontología de Vertebrados, Fundación-Instituto Miguel Lillo, Universidad Nacional de Tucumán, San Miguel de Tucumán, Tucumán (Argentina); **TMM**, Vertebrate Paleontology Laboratory, Texas Natural Science Center, Austin, TX (USA); **ULBRA**, Universidade Luterana do Brasil, Coleção de Paleovertebrados, Canoas, Rio Grande do Sul (Brazil).

Micro-computed tomography acquisition and image processing

This work is based on seven individuals (the holotype NHMUK PV R3556, the two individuals in NHMUK RV R3146, NHMUK PV R3914, NHMUK PV R4823/4, NHMUK PV R5589) referred to *Scleromochlus taylori*. All of them were subjected to µCT scanning. Because each specimen is embedded in broken sandstone blocks consisting of multiple parts, these blocks were first re-assembled and held together with rubber bands before µCT scanning started. This additional step was necessary to: capture the specimens in their entirety

in a single scan; to minimise the risk of misidentification of individual elements that have been broken into separate sections and preserved in different parts of the original articulated blocks (e.g. the humerus in NUMUK PV R3556); and to improve measurement accuracy[14]. Five specimens (NHMUK PV R3556, NHMUK RV R3146, NHMUK PV R3914, NHMUK PV R4823/4, NHMUK PV R5589) were scanned at the Imaging and Analysis Centre of the NHMUK, using the Nikon XT H 225 by Dr Vincent Fernandez with the assistance of PMB. NHMUK PV R3557 was scanned at the Palaeobiology Lab of the University of Bristol by Dr Tom G. Davis with the assistance of Dr Elizabeth G. Martin-Silverstone using a Nikon XT H 225. The µCT scans and their parameters are freely available in MorphoSource alongside videos of the complete digital models (see Data availability), following community recommendations for the availability of digital data[46].

The µCT data were processed and segmented using Mimics Research v22.0[47]. We additionally checked and, where possible confirmed, our observations on multiple generations of casts and moulds of the same specimens. DF and PMB worked with the peels in the collections of NHMUK, while SJN worked on additional peels made by Kevin Padian in the 1980s and then cast in epoxy by Marilyn Fox (YPM); this set of casts is currently located with SJN at Virginia Tech.

Phylogenetic analyses

Using our new anatomical data, *Scleromochlus taylori* was scored for ~40–42% of the character states in the phylogenetic data matrix of Ezcurra *et al.*[7]. This more than doubles the information available for this taxon in the previous version of the dataset, and makes *Scleromochlus* one of the most completely scored Triassic avemetatarsalians. We used this dataset[7], which is an expanded version of the matrix in reference[19], because it contains the most comprehensive sample of Permian–Triassic archosauromorphs available and includes

the most relevant character states and taxa to appropriately test all of the historical hypotheses concerning the relationships of *Scleromochlus*.

The final dataset includes 822 characters and 158 terminal taxa. Following previous works, 36 undiagnostic and/or problematic operational taxonomic units (OTUs), and some that were scored solely for the purpose of disparity analyses, were excluded *a priori* (references[7,48–50] for further justifications regarding these exclusions) (i.e. *Dinocephalosaurus orientalis, Fuyuansaurus acutirostris, Pectodens zhenyuensis, Protanystropheus antiquus, Trachelosaurus fischeri, Tanystropheus haasi, Malerisaurus robinsonae, Arctosaurus osborni, Eorasaurus olsoni, Prolacertoides jimusarensis, Archosaurus rossicus* (complete), Panchet proterosuchid, *Vonhuenia fredericki, Chasmatosuchus rossicus* (combined), *Chasmatosuchus magnus* (combined), *Chasmatosuchus vjushkovi, Koilamasuchus gonzalezdiazi, Kalisuchus rewanensis* (holotype), NMQR 3570, *Shansisuchus kuyeheensis, Uralosaurus* (combined), *Osmolskina czatkoviensis, Osmolskina* (complete), *Triopticus primus, Angistorhinus talainti,* Otter Sandstone Formation Archosaur, *Dagasuchus santacruzensis, Hypselorhachis mirabilis, Waldhaus poposauroid, Vytshegdosuchus zbeshartensis, Bystrowisuchus flerovi, Bromsgroveia walkeri,* Moenkopi Formation poposauroid, *Lutungutali sitwensis, Nyasasaurus parringtoni*). *Petrolacosaurus kansensis* was selected as the outgroup. The following characters were treated as additive: 1, 2, 7, 10, 17, 19–21, 28, 29, 36, 40, 42, 46, 50, 54, 66, 71, 74–76, 122, 127, 146, 153, 156, 157, 171, 176, 177, 187, 202, 221, 227, 263, 266, 278, 279, 283, 324, 327, 331, 337, 345, 351, 352, 354, 361, 365, 370, 377, 379, 386, 387, 398, 410, 414, 424, 430, 435, 446, 448, 454, 455, 458, 460, 463, 470, 472, 478, 482, 483, 485, 489, 490, 502, 504, 510, 516, 521, 529, 537, 546, 552, 556, 557, 567, 569, 571, 574, 581, 582, 588, 636, 648, 652, 662, 701, 731, 735, 737, 738, 743, 749, 766, 784 and 816 (taxon-character matrix).

Three different ankle interpretations were scored in different *Scleromochlus taylori* OTUs, plus an additional one where all ambiguous ankle characters were left unscored. To explicitly test how the ankle interpretation affects the position of *Scleromochlus* in the phylogeny we ran a different phylogenetic analysis for each of these. In each analysis only a single *Scleromochlus* OTU was kept active.

Maximum parsimony. Maximum parsimony analyses were performed in TNT 1.5[51–52] using equally weighted parsimony. A tree space was generated and searches for the most parsimonious trees (MPTs) were conducted using a similar protocol to that in ref.[7]: the tree-search algorithm Wagner trees, tree bisection and reconnection (TBR) branch swapping, and New Technology search (Sectorial Search, Ratchet, Drift and Tree fusing) until 100 optimal hits were reached. This was followed by a final round of tree bisection reconnection (TBR) branch swapping, with a 50% collapsing rule. Consistency Index (CI) and Retention Index (RI) were calculated using the script statsB.run[51], which, unlike stats.run[52–53], does not include deactivated terminals when calculating CI and RI[51]. Branch support was calculated using bootstrap resampling analyses, with 1,000 technical pseudo-replicates for both absolute and group present/contradicted (GC) frequencies, and Bremer support.

Bayesian inference analysis. We conducted Bayesian tip-dating analysis using MrBayes (3.2.7)[54] and repeated it for all the interpretations of *Scleromochlus* ankle anatomy. Our analysis was run with the same settings as the unconstrained version of ref.[7]. We ran a Markov k-state variable substitution using the same set of characters as in the maximum parsimony analysis. No topological constraint was applied to the tree, only some time constraints to specific nodes: uniform age priors and gamma-rate relaxed clock models were modelled on First and Last Appearance Dates (FAD and LAD) for all tips of the tree; the oldest split of the tree was set a 304.4–318 Mya and was based on the age of earliest occurrence of crown-amniotes in the Joggings Formation[55], and the estimated age of

Petrolacosaurus kansensis; the node age calibration of Archosauria was set with a uniform prior at 249.2–257.4 Mya, respectively, based on the oldest archosaur in the fossil record, and the age estimate of the archosaur–squamate lines split (see[49,56]). All tips were specified to be fossils, in a fossilised birth–death process under standard parametrization. All analyses ran Metropolis-coupling Markov chain Monte Carlo algorithm, two runs of four chains each with a heat coefficient of 0.05 and three swap attempts per generation.

Systematic Palaeontology

Archosauria Cope, 1869

Avemetatarsalia Benton, 1999

Ornithodira Gauthier, 1986

P**terosauromorpha** Padian, 1997

Scleromochlus taylori Woodward, 1907

Holotype. NHMUK PV R3556, an almost complete impression of a skeleton in sandstone split into four blocks. Some additional elements (pedal phalanges, ribs and caudal vertebrae) are only visible in the μCT scans because they are still completely embedded in the sandstone matrix.

Referred material. NHMUK PV R3557; NHMUK PV R3146 (two individuals); NHMUK PV R3914; NHMUK PV R4823/4; NHMUK PV R5589 all of which are partial to complete impressions of skeletons preserved in sandstone similarly to the type specimen, and with variable numbers of elements still embedded in the sandstone matrix.

Locality and horizon. All specimens were collected from the Lossiemouth East Quarry in Lossiemouth near Elgin (Moray, Scotland, United Kingdom), except NHMUK PV R5589, which was recovered from the West Quarry of the same location. All of the

specimens come from the aeolian sandstone deposits of the Lossiemouth Sandstone Formation (Late Triassic: ~late Carnian/early Norian) (see[5,13,56] and refer to[7,48–49, 56–58] for comments on the biostratigraphic correlations of the Lossiemouth Sandstone Formation with other Late Triassic formations).

Diagnosis. *Scleromochlus taylori* is a small-bodied, gracile pterosauromorph avemetatarsalian with the following unique combination of character states (autapomorphies denoted by an asterisk): * retroarticular process of the mandible moderately expanded posteriorly, with a distal end that is weakly expanded dorsolaterally-to-ventromedially; * parietal with a transverse posterolateral process; anterior cervical with transversely convex ventral surface; * middle and posterior dorsal vertebrae with an elongated centrum (height/length ratio > 2.5); straight (i.e. not sigmoidal) humerus; gracile humerus (present in some trees) with a maximum proximal transverse width /total length ratio ~0.16 to 0.2; * short deltopectoral crest, reaching only 15–18% of the humeral length; short pubis, <30% of the total length of the femur; narrow femur distal transverse width, ~11% of the total length; short metacarpal, <10% of the length for the humerus and only ~18% the length than the longest metatarsals; metatarsals I–IV equal in length (shared with pterosaurs but not lagerpetids).

Data availability

The taxon/character data matrices for the phylogenetic analyses for TNT and MrBayes are available in Nexus and TNT formats in the SI and in MorphoBank at https://morphobank.org/index.php/Projects/ProjectOverview/project_id/4327. The µCT datasets and videos of the six specimens of *Scleromochlus taylori* are available in MorphoSource https://www.morphosource.org/projects/000414456/?locale=en (the videos are also available as SI files).

585

586 46. Davies, T. G., Rahman, I. A., Lautenschlager, S., Cunningham, J. A., Asher, R. J.,
587 Barrett, P. M., Bates, K. T., Bengtson, S., Benson, R. B. J., Boyer, D. M., Braga, J.,
588 Bright, J. A., Claessens, L. P. A. M., Cox, P. G., Dong, X.-P., Evans, A. R.,
589 Falkingham, P. L., Friedman, M., Garwood, R. J., Goswami, A., Hutchinson, J. R.,
590 Jeffery, N. S., Johanson, Z., Lebrun, R., Martínez-Pérez, C., Marugán-Lobón, J.,
591 O'Higgins, P. M., Metscher, B., Orliac, M., Rowe, T. B., Rücklin, M., Sánchez-
592 Villagra, M. R., Shubin, N. H., Smith, S. Y., Starck, J. M., Stringer, C., Summers, A.
593 P., Sutton, M. D., Walsh, S. A., Weisbecker, V., Witmer, L. M., Wroe, S., Yin, Z.,
594 Rayfield, E. J. & Donoghue, P. C. J. Open data and digital morphology. *Proc. Royal*
595 *Soc. B* **284**, 20170194 (2017).
596 47. https://www.materialise.com/mimics
597 48. Ezcurra, M.D., Fiorelli, L.E., Martinelli, A.G., Rocher, S., Von Baczko, M.B.,
598 Ezpeleta, M., Taborda, J.R., Hechenleitner, E.M., Trotteyn, M.J., Desojo, J.B. 2017.
599 Deep faunistic turnovers preceded the rise of dinosaurs in southwestern Pangaea. *Nat.*
600 *Ecol. Evol.* **1(10)**, 1477–1483 (2017).
601 49. Ezcurra, M.D., Butler, R.J. The rise of the ruling reptiles and ecosystem recovery
602 from the Permo-Triassic mass extinction. *Proc. Royal Soc. B* **285**, 20180361 (2018).
603 50. Butler, R.J., Sennikov, A.G., Dunne, E.M., Ezcurra, M.D., Hedrick, B.P., Maidment,
604 S.C.R., Meade, L.E., Raven, T.J., Gower, D.J. Cranial anatomy and taxonomy of the
605 erythrosuchid archosauriform '*Vjushkovia triplicostata*' Huene, 1960, from the Early
606 Triassic of European Russia. *R. Soc. Open Sci.* **6**, 191289 (2019).
607 51. Spiekman, S.N.F., Ezcurra, M.D., Butler, R.J., Fraser, N.C., Maidment, S.C.R.
608 *Pendraig milnerae,* a new small-sized coelophysoid theropod from the Late Triassic
609 of Wales. *R. Soc. Open Sci.* **8**, 210915 (2021).

52. Goloboff, P.A., Farris, J.S., Nixon, K.C. TNT, a free program for phylogenetic analysis. *Cladistics* **24**, 774–786 (2008).
53. Goloboff, P.A., Catalano, S.A. TNT version 1.5, including a full implementation of phylogenetic morphometrics. *Cladistics* 32, 221–238 (2016).
54. Ronquist, F., van der Mark, P., Huelsenbeck, J.P. In The Phylogenetic Handbook: a Practical Approach to Phylogenetic Analysis and Hypothesis Testing (eds Lemey, P. et al) 210–266 (Cambridge Univ. Press, 2009) (2009).
55. Benton, M.J., Donoghue, P.C.J., Asher, R.J., Friedman, M., Near, T.J., Vinther, J. Constraints on the timescale of animal evolutionary history. *Palaeontol. Electronica* 18, 1–106 (2015).
56. Ezcurra, M.D., Scheyer, T.M., Butler, R.J. The origin and early evolution of Sauria: reassessing the Permian saurian fossil record and the timing of the crocodile-lizard divergence. *PLoS ONE* 9, e89165 (2014).
57. Benton, M.J., Walker, A.D. *Erpetosuchus*, a crocodile-like basal archosaur from the Late Triassic of Elgin, Scotland. *Zoological Journal of the Linnean Society* 136, 25–47 (2002).
58. Bernardi, M., Gianolla, P., Petti, F.M., Mietto, P., Benton, M.J. Dinosaur diversification linked with the Carnian Pluvial Episode. *Nature Communication*, 9, 1499 (2018). https://doi.org/10.1038/s41467-018-03996-1

Acknowledgments First and foremost, we thank Dr Vincent Fernandez (NHMUK), Dr Tom G. Davies (UoB) and Dr Elizabeth G. Martin-Silverstone (UoB) for scanning the specimens. Our gratitude also goes to Dr Alessandro A. Chiarenza for discussion and assistance. We thank Gabriel Ugueto for creating the artwork that accompanies this manuscript and Matt Humpage for the 3D reconstruction of the skeleton. We thank Adam Fitch for sharing the photograph of *Raeticodactylus* used in Figure 2 and Scott Hartman

for permission to use silhouettes from phylopic.org. Finally, we would like to thank the reviewers Dr Martin Ezcurra, Prof Kevin Padian, Prof Lawrence Tanner, Dr Hans-Dieter Sues, an anonymous referee, and the Editor Dr Henry Gee whose insightful comments greatly improved the quality of this manuscript. This study was supported by the Royal Commission for the Exhibition of 1851 – Science Fellowship awarded to D.F.. R.J.B., E.M.D., A.F., D.J.L., and P.J.V. were supported by a Leverhulme Research Project Grant (RPG-2019-365).

Author Contributions D.F. designed the project with inputs of N.C.F., S.W., R.J.B., P.M.B.; S.L.B. and S.J.N.; D.F. processed the μCT data and described the material; D.F., with the assistance of S.J.N. and P.M.B., scored the phylogenetic matrices and conducted the phylogenetic analyses; D.F. wrote the bulk of the manuscript and made the figures; P.M.B. conducted sedimentological tests on the specimens. All authors contributed to the writing, discussions and conclusions.

Competing interests. The authors declare no competing interests.

Additional Information

Supplementary Information is available for this paper at [to be completed]

Correspondence and requests for materials should be addressed to D.F.

Peer review information Nature thanks Dr Martin Ezcurra, Prof. Kevin Padian, Prof. Lawrence Tanner, Dr Hans-Dieter Sues, and an anonymous referee for their contributions to the peer review of this work. Peer reviewer reports are available.

Reprints and permissions information is available at http://www.nature.com/reprints.

Extended Data

Extended Data Figure 1. Life reconstruction of *Scleromochlus taylori*. Artwork by Gabriel Ugueto (high-resolution version).

Extended Data Figure 2. Digital rendering of *Scleromochlus taylori* specimens from µCT scans. Holotype NHMUK PV R3556, dorsal view (top left); NHMUK PV R3557, ventral view (right); NHMUK PV R3914, ventral view (bottom left). Red shading highlights the skeleton traces on the digital peels, while solid red rendering indicates previously unknown body parts.

Extended Data Figure 3. Strict consensus phylogenetic tree of analysis including indeterminate ankle scores. Absolute and present/contradicted group bootstrap frequencies (respectively left and right above the branches) and Bremer support values (below the branches). Note that in ~95% of the most parsimonious trees *Scleromochlus* is found as the earliest-diverging lagerpetid (it is alternatively found as the earliest-diverging member of a lagerpetid clade also composed of *Ixalerpeton*, *Kongonaphon* and *Lagerpeton*).

Extended Data Figure 4. Strict consensus phylogenetic tree of analysis using scores for an advanced fused mesotarsal ankle. Absolute and present/contradicted group bootstrap frequencies (respectively left and right above the branches) and Bremer support values (below the branches). Note that in ~95% of the most parsimonious trees *Scleromochlus* is found as the earliest-diverging lagerpetid (it is alternatively found as the earliest-diverging member of a lagerpetid clade also composed of *Ixalerpeton*, *Kongonaphon* and *Lagerpeton*).

Extended Data Figure 5. Strict consensus phylogenetic tree of analysis using scores for an "intermediate" mesotarsal ankle. Absolute and present/contradicted group bootstrap frequencies (respectively left and right above the branches) and Bremer support values (below the branches).

Extended Data Figure 6. Strict consensus phylogenetic tree of analysis based on scores for a crurotarsal ankle. Absolute and present/contradicted group bootstrap frequencies (respectively left and right above the branches) and Bremer support values (below the branches).

Extended Data Figure 7. Bayesian inference convergence topology trees. The position of *Scleromochlus taylori* remains the same regardless of the scoring strategy of the ankle. The alternative topology within Pterosauria is found only when using the 'crurotarsal ankle' settings.

Extended Data Table 1. Table of measurements. Measurements (maximum length in mm) of *Scleromochlus taylori* individuals. i, incomplete; e, estimated; ---, not available.

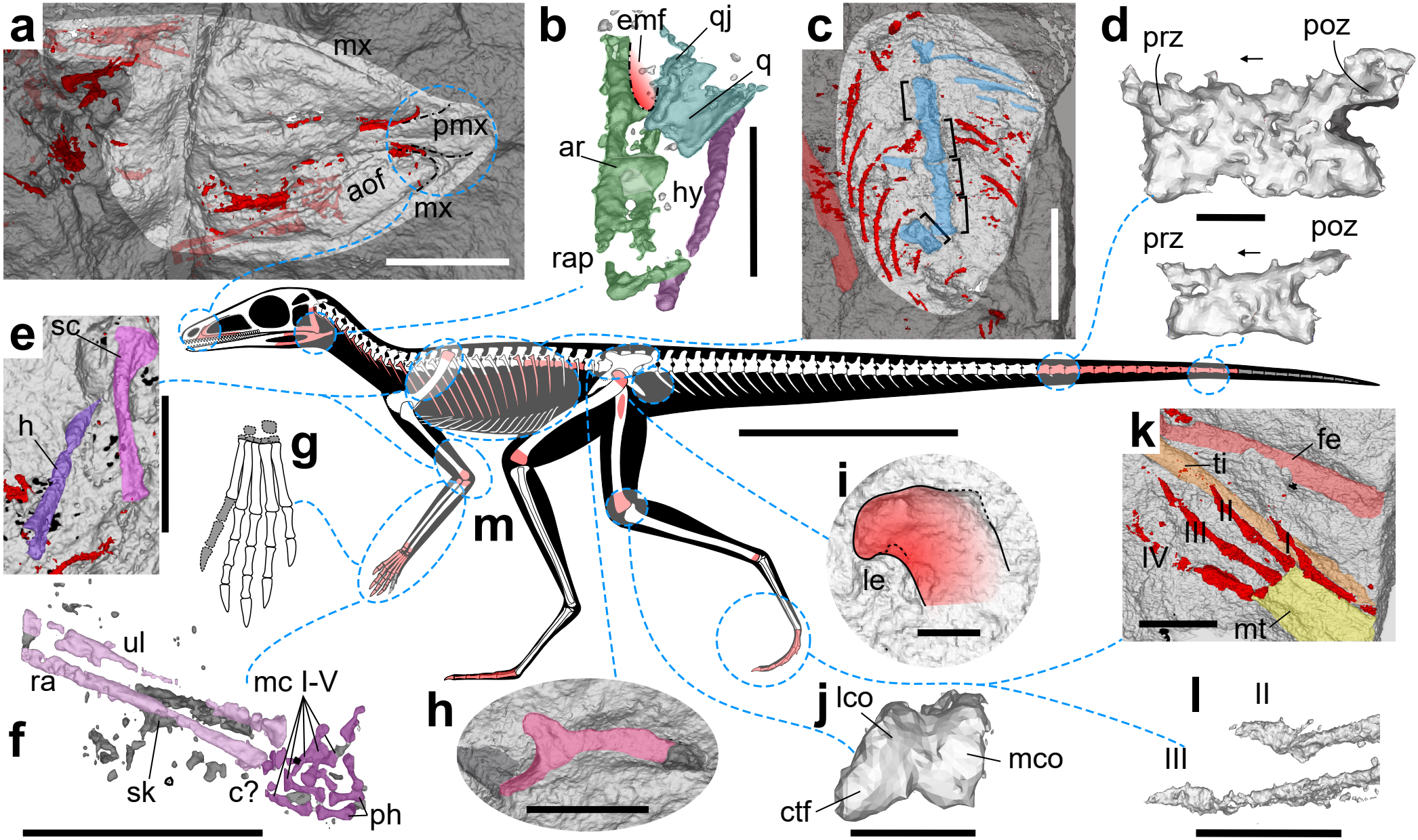
a
mx
pmx
aof
mx
b
emf
qj
q
ar
hy
rap
c
d
prz
poz
prz
poz
e
sc
h
g
m
i
le
k
fe
ti
II
III
IV
I
mt
f
ul
ra
mc I-V
sk
c?
ph
h
j
lco
mco
ctf
l
II
III

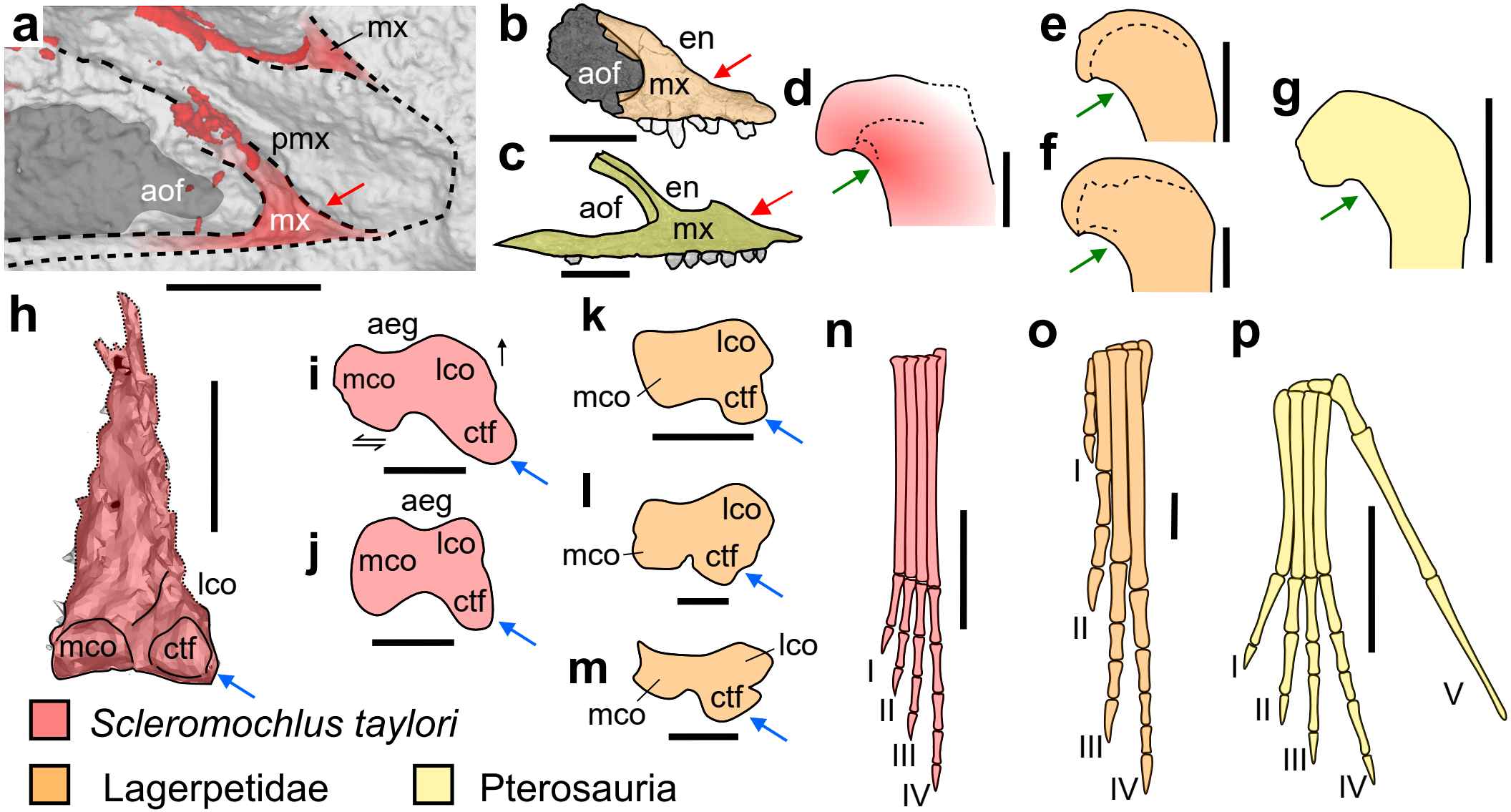
a
mx
pmx
aof
mx
b
aof
en
mx
c
aof
en
mx
d
e
f
g
h
lco
mco
ctf
i
aeg
mco
lco
ctf
j
aeg
mco
lco
ctf
k
lco
mco
ctf
l
lco
mco
ctf
m
lco
mco
ctf
n
I
II
III
IV
o
I
II
III
IV
p
I
II
III
IV
V
Scleromochlus taylori
Lagerpetidae
Pterosauria

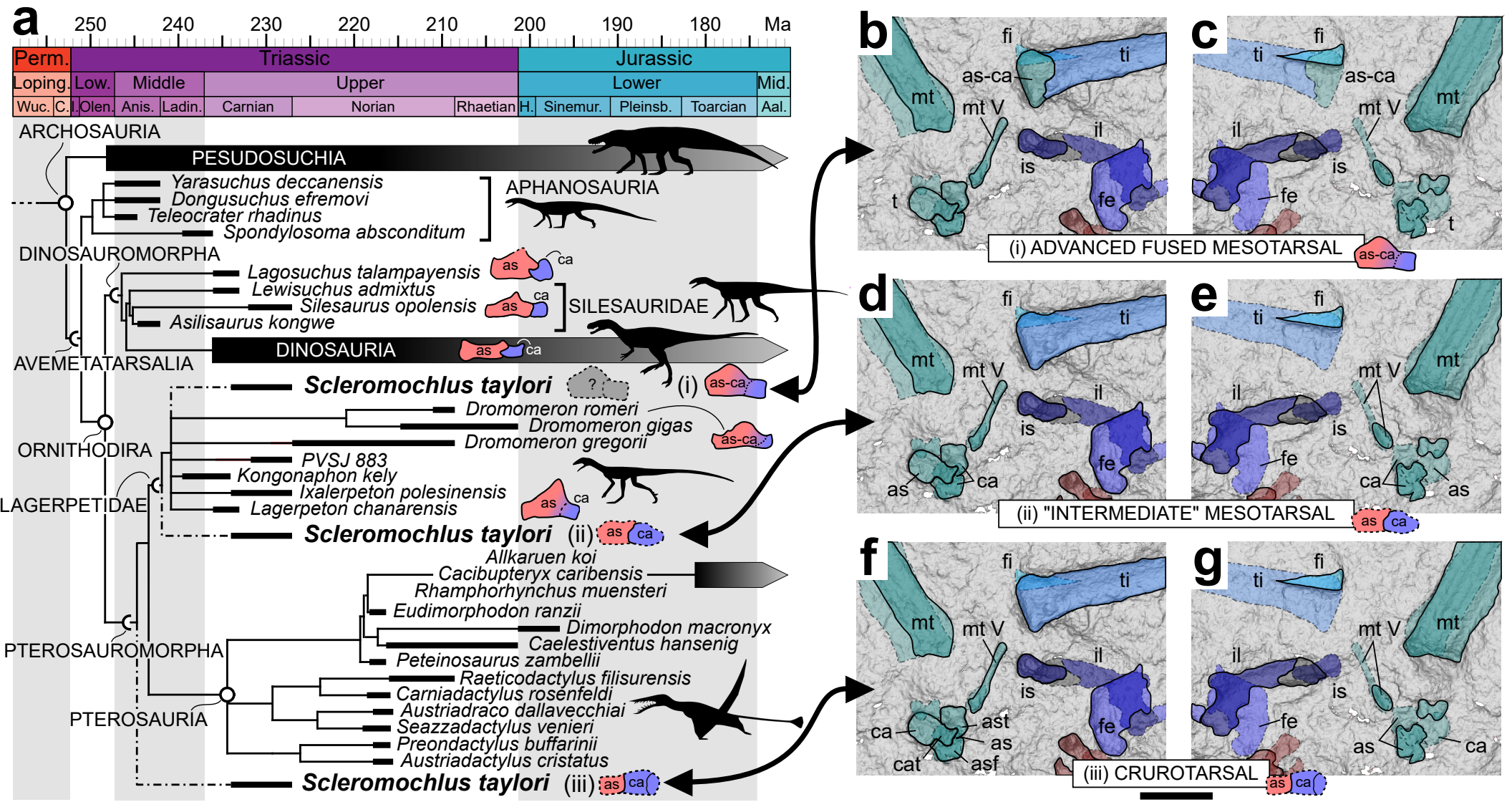
a
250
240
230
220
210
200
190
180
Ma
Perm.
Triassic
Jurassic
Loping.
Low.
Middle
Upper
Lower
Mid.
Wuc.
C.
I.
Olen.
Anis.
Ladin.
Carnian
Norian
Rhaetian
H.
Sinemur.
Pleinsb.
Toarcian
Aal.
ARCHOSAURIA
PESUDOSUCHIA
Yarasuchus deccanensis
Dongusuchus efremovi
Teleocrater rhadinus
Spondylosoma absconditum
APHANOSAURIA
DINOSAUROMORPHA
Lagosuchus talampayensis
Lewisuchus admixtus
Silesaurus opolensis
Asilisaurus kongwe
SILESAURIDAE
DINOSAURIA
AVEMETATARSALIA
Scleromochlus taylori
(i)
ORNITHODIRA
Dromomeron romeri
Dromomeron gigas
Dromomeron gregorii
PVSJ 883
Kongonaphon kely
Ixalerpeton polesinensis
Lagerpeton chanarensis
LAGERPETIDAE
Scleromochlus taylori
(ii)
Allkaruen koi
Cacibupteryx caribensis
Rhamphorhynchus muensteri
Eudimorphodon ranzii
Dimorphodon macronyx
Caelestiventus hansenig
Peteinosaurus zambellii
PTEROSAUROMORPHA
Raeticodactylus filisurensis
Carniadactylus rosenfeldi
Austriadraco dallavecchiai
Seazzadactylus venieri
Preondactylus buffarinii
Austriadactylus cristatus
PTEROSAURIA
Scleromochlus taylori
(iii)
as
ca
as-ca
b
c
d
e
f
g
fi
ti
mt
mt V
il
is
fe
t
ca
as
ast
cat
asf
(i) ADVANCED FUSED MESOTARSAL
(ii) "INTERMEDIATE" MESOTARSAL
(iii) CRUROTARSAL


a
b